

Portable system integrated with time comparison, ranging, and communication

Qionqiong Zhang (章琼琼)¹, Chengkai Pang (庞程凯)^{1,2}, Yurong Wang (王煜蓉)^{1,2}, Guangyue Shen (申光跃)^{1,2}, Lei Yang (杨雷)¹, Zhaohui Li (李召辉)¹, Haiyan Huang (黄海燕)¹, and Guang Wu (吴光)^{1,2,3*}

¹State Key Laboratory of Precision Spectroscopy (East China Normal University), Shanghai 200241, China

²Chongqing Key Laboratory of Precision Optics, Chongqing Institute of East China Normal University, Chongqing 401120, China

³Collaborative Innovation Center of Extreme Optics, Shanxi University, Taiyuan 030006, China

*Corresponding author: gwu@phy.ecnu.edu.cn

Received February 11, 2022 | Accepted May 25, 2022 | Posted Online June 25, 2022

We demonstrate a portable system integrated with time comparison, absolute distance ranging, and optical communication (TRC) to meet the requirements of space gravitational wave detection. A 1 km free-space asynchronous two-way optical link is performed. The TRC realizes optical communication with 7.7×10^{-5} bit error rate with a Si avalanche photodiode single-photon detector, while the signal intensity is 1.4 photons per pulse with the background noise of 3×10^4 counts per second. The distance measurement uncertainty is 48.3 mm, and time comparison precision is 162.4 ps. In this TRC system, a vertical-cavity surface-emitting laser diode with a power of 9.1 μ W is used, and the equivalent receiving aperture is 0.5 mm. The TRC provides a miniaturization solution for ultra-long distance inter-satellite communication, time comparison, and ranging for space gravitational wave detectors.

Keywords: gravitational waves detection; time comparison; optical communication; ranging.

DOI: [10.3788/COL202220.100601](https://doi.org/10.3788/COL202220.100601)

1. Introduction

In 1915, Albert Einstein proposed the general theory of relativity and then predicted the existence of gravitational waves in 1916^[1]. Until September 14, 2015, the Laser Interferometer Gravitational Wave Observatory (LIGO) disclosed the results of gravitational wave detection, which was the first time, to the best of our knowledge, in human history to directly detect gravitational wave signals, opening a new window for human beings to understand the universe^[2]. Due to the influence of ground vibration and limited interference arm length on ground, space gravitational wave detection has become an international popular research field^[3–8]. The Laser Interferometer Space Antenna (LISA) project, jointly proposed by European Space Agency (ESA) and National Aeronautics and Space Administration (NASA) in the 1990s, is a representative space gravitational wave program^[9]. LISA planned to form a regular triangle constellation operating in solar orbit in order to construct a large laser interferometer in space^[10–12]. LISA Pathfinder, a LISA technology verification star, was successfully launched in 2015, opening a new era of space gravitational wave detection^[13]. In addition, Chinese researchers proposed the Taiji project for space gravitational wave detection, which is expected to launch three satellites to form an equilateral triangle with an arm length of 3

million kilometers in space^[14–16]. Among these typical space gravitational wave detection missions, time delay interferometry (TDI) is an important technique for laser frequency noise subtraction. This technique requires additional measurements: inter-satellite absolute distance measurement, inter-satellite optical communication, and time comparison. As for LISA, the absolute distance measurement accuracy between the spacecraft is about 1 m, and the clock offset between spacecraft is a few nanoseconds^[17]. Some functions of TDI technology have completed the principle demonstration in the laboratory, consuming more than 10% of the laser power^[18–22]. Space resources and laser power are very precious in space gravitational wave detection, and thus a portable integration system that is highly sensitive and multifunctional is required.

In order to meet the application requirements of the space gravitational wave detection mission, a portable integration system of time comparison, optical ranging, and communication (TRC) is invented based on single-photon detection. An asynchronous two-way optical link is constructed, and the signal loss can be reduced from proportional to R^4 to proportional to R^2 compared with the one-way link and corner-reflector-based two-way link, where R represents the distance between two terminals^[23]. The TRC system adopts the single-photon direct detection mode to simplify the design, reduce the load, and

improve the sensitivity. In the system based on single-photon detection, the time comparison precision can reach the order of picoseconds^[24,25], the ranging uncertainty can reach the order of centimeters^[26,27], and the bit error rate (BER) of optical communication is in the order of 10^{-3} to 10^{-6} ^[28,29]. In this paper, a 1.05 km free-space link is constructed. The optical communication is realized with the data rate of ~ 195.3 kbit/s and the BER of 7.7×10^{-5} , under the condition of 3×10^4 counts per second (cps) background noise and the signal light intensity of 1.4 photons per pulse at the receiver. In addition, the ranging uncertainty is 48.3 mm, and the precision of time comparison is 162.4 ps. To the best of our knowledge, this portable and highly sensitive TRC realizes the integrated demonstration of TRC based on single-photon detection for the first time, which provides a technique for space gravitational wave detectors.

2. Methods

2.1. Asynchronous two-way optical link

The TRC integration system is an asynchronous two-way link, and the schematic is shown in Fig. 1. There are two identical systems located at site A and site B. The laser diode (LD) in system A (LD_A) is triggered by signals modulated by a field programmable gate array (FPGA) modulator and transmits optical signals carrying start of frame (SF), t_1 , communication information, and end of frame (EF) to system B, where t_1 is the transmitting time of the first pulse in one frame of data. The single-photon detector (SPD) in system B (SPD_B) receives optical signals transmitted by A and stores them through $FPGA_B$. The arriving time of the first pulse in one frame of data is recorded as t_2 . Communication information and t_1 can be obtained by demodulation, and t_2 can be obtained by time to digital convertor (TDC) in $FPGA_B$. Similarly, we get t_3 and t_4 . The information sent by A includes t_3 , and that sent by B includes t_1 . Match the above adjacent time measurement events, and then obtain a series of asynchronous two-way events: $[t_1, t_2, t_3, t_4]$. Without considering the internal delay difference between the systems on both sides, the channel delay can be considered as $d_{AB} = d_{BA}$ because the signal passes through the same path. Suppose sites A and B are relatively stationary, the time of A and B is provided by the same clock. The time difference τ between A and B can be expressed as

$$\tau = (t_2 + t_3 - t_1 - t_4)/2. \quad (1)$$

The distance R between sites A and B can be calculated from

$$R = \frac{c}{2} [(t_4 - t_1) - (t_3 - t_2)], \quad (2)$$

where c is the speed of light.

2.2. Analysis of coding/decoding

The TRC system uses pseudo-random (PN) code to the spread spectrum, and the PN code adopts the m sequence, which is generated by a linear feedback shift register (LFSR). A five-stage LFSR is adopted in this scheme with the initial state $(a_4, a_3, a_2, a_1, a_0) = (0, 1, 0, 0, 1)$, and the primitive polynomial is

$$f(x) = x^5 + x^2 + 1. \quad (3)$$

The schematic of the m -sequence generator is shown in Fig. 2(a), and the working state of five-stage LFSR is shown in Table 1. In order to facilitate later data processing, we complement "0" after the m sequence to make the period of the PN code 2^5 . The period of the PN code is 32 chips in this system, and the sequence is 10010000101011101100011111001100. The number of 0 and 1 is equal in the PN code sequence, and the autocorrelation peak appears when SF and EF are aligned. Otherwise, the autocorrelation peak is close to zero. The process of data decoding is shown in Fig. 2(b). $FPGA_B$ records the pulse arrival time

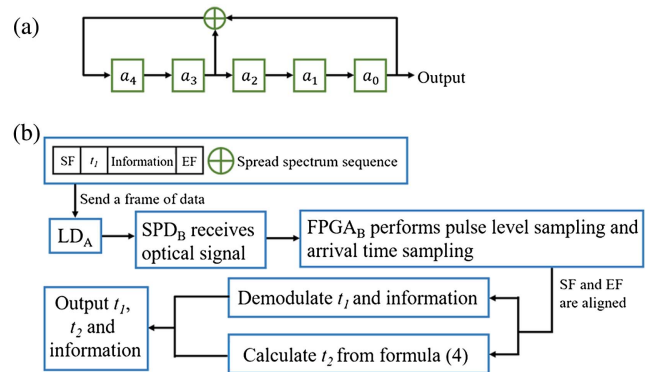


Fig. 2. (a) Schematic of m -sequence generator. (b) Flow chart of data decoding process.

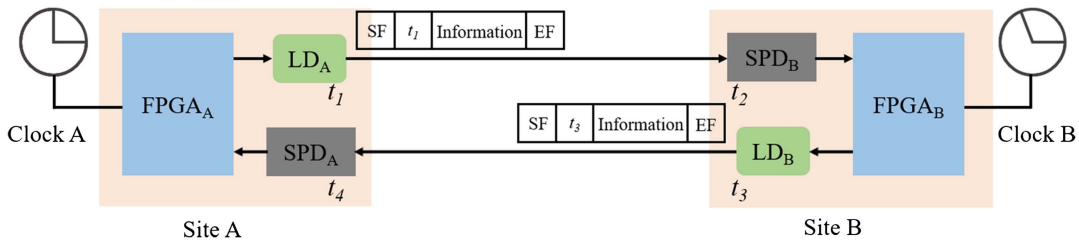


Fig. 1. Schematic of asynchronous two-way optical link. SPD, single-photon detector; LD, laser diode; SF, start of frame; EF, end of frame; FPGA, field programmable gate array.

Table 1. Working State of Five-Stage Linear Feedback Shift Register.

a_4	a_3	a_2	a_1	a_0	Out	a_4	a_3	a_2	a_1	a_0	Out
0	1	0	0	1	1	0	0	0	1	1	1
0	0	1	0	0	0	1	0	0	0	1	1
0	0	0	1	0	0	1	1	0	0	0	0
0	0	0	0	1	1	1	1	1	0	0	0
1	0	0	0	0	0	1	1	1	1	0	0
0	1	0	0	0	0	1	1	1	1	1	1
1	0	1	0	0	0	0	1	1	1	1	1
0	1	0	1	0	0	0	0	1	1	1	1
1	0	1	0	1	1	1	0	0	1	1	1
1	1	0	1	0	0	1	1	0	0	1	1
1	1	1	0	1	1	0	1	1	0	0	0
0	1	1	1	0	0	1	0	1	1	0	0
1	0	1	1	1	1	0	1	0	1	1	1
1	1	0	1	1	1	0	0	1	0	1	1
0	1	1	0	1	1	1	0	0	1	0	0
0	0	1	1	0	0						

and starts level sampling when SPD_B receives the optical signal. The transmitting time t_1 of the first pulse in one frame of data of LD_A and the communication information can be demodulated when SF and EF are aligned. Due to the error of single-time measurement, we improve the measurement accuracy of the arriving time t_2 of the first pulse in one frame of data by averaging the arrival times of multiple pulses. Suppose there are N pulses in a frame of data, and the arrival time of each pulse is recorded as t'_n ($n = 1, 2, \dots, N$); t_2 can be calculated by

$$t_2 = \frac{1}{N} \sum_{n=1}^N \left(t'_n - \left[\frac{t'_n - t'_1}{T_s} \right] \cdot T_s \right), \quad (4)$$

where T_s represents the sampling time of the single code, and $[(t'_n - t'_1)/T_s]$ is an integer function. We get t_3 and t_4 in the same way, and a group of time events $[t_1, t_2, t_3, t_4]$ can be obtained. Finally, time difference and distance between sites A and B are calculated from Eqs. (1) and (2).

In the decoding process, an SPD is used to improve the sensitivity of the system, which conforms to the Poisson distribution. For one SPD with detection efficiency η , dead time T_d , and dark count rate C_d , the probability of signal detection P_s and noise detection P_b can be expressed as

$$P_s = e^{-T_d(C_d+C_b)} \cdot (1 - e^{-\mu}), \quad (5)$$

$$P_b = 1 - e^{-T_s(C_d+C_b)}, \quad (6)$$

where C_b is the count rate of background light, T_s represents the sampling time of single code, and μ is the average photon number per pulse. The transmission code is obtained by adding the signal code and PN code by module 2. The 0 code and 1 code are added with the PN code by module 2, and two different sequences are obtained. Comparing the acquisition sequence with these two sequences, the signal code is demodulated by coincidence analysis. For the PN code with period length of M chips, the BER of this system can be expressed as

$$\text{BER} = 1 - \left[\sum_{i=1}^{\frac{M}{2}} P_s^i (1 - P_s)^{\frac{M}{2}-i} \cdot \sum_{j=\frac{M}{2}+1-i}^{\frac{M}{2}} (1 - P_b)^j P_b^{\frac{M}{2}-j} + \frac{1}{2} \sum_{k=0}^{\frac{M}{2}} P_s^k (1 - P_s)^{\frac{M}{2}-k} (1 - P_b)^{\frac{M}{2}-k} P_b^k \right]. \quad (7)$$

3. Experimental Setup and Results

To verify the possibility of the TRC integration system, we constructed a free-space asynchronous two-way link over 1 km. As shown in Fig. 3(a), the link is actually a folded atmosphere link. Two identical setups are located at sites A and B on the same side, respectively. The 850 nm LD is triggered by signals modulated by the FPGA modulator (Xilinx, XC7A35TFGG484-2). The angle of the laser after passing through the variable optical attenuator (VOA) and collimator (COL) is adjusted by a mirror (M) and incident on a plane M with a diameter of 101.6 mm on the other side. The reflected light is detected by a self-developed Si avalanche photodiode SPD (Si SPAD) with an active area of 500 μm in diameter at another site after passing through a filter (F). The clocks of A and B are provided by the same crystal oscillator. The setup was located at the Lanxiang Lake in Shanghai for field experiment, and the photograph is shown in Fig. 3(b). The SPD was put in a dark room in order to reduce the influence of background noise. The distance from the plane M to the two sites is ~ 520 m. The whole link realizes time comparison, absolute distance measurement, and optical communication at the kilometer level.

The TDC used in the TRC system was self-developed by our research group based on an FPGA board with a time resolution of about 91 ps. The precision of the TDC was tested to verify whether the TDC can meet the time measurement requirements of the system. The signal generator generated two signals. The first arrival signal was used as the start signal, and the second arrival signal was used as the stop signal. The TDC recorded the time interval between the two signals. The precision of the TDC is uncertain due to the influence of the internal noise, so the standard deviation of a large number of measured values at fixed time intervals under the same conditions is taken as the standard to measure the precision. The measurement results are

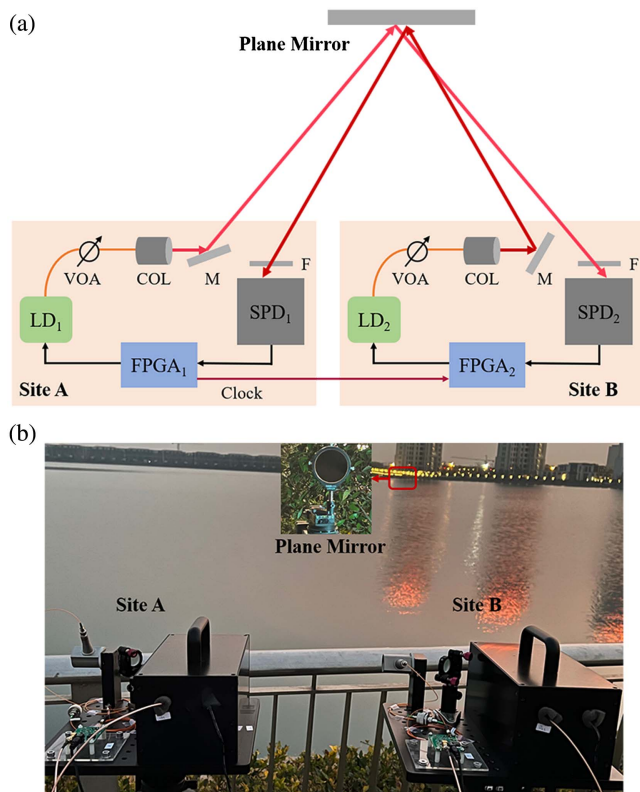


Fig. 3. (a) Schematic of asynchronous two-way optical link. (b) System takes place at the Lanxiang Lake, Shanghai. SPD, single-photon detector; LD, laser diode; FPGA, field programmable gate array; F, filter; M, mirror; VOA, variable optical attenuator; COL, collimator.

shown in Fig. 4, and the precision of the TDC was 67.7 ps. In the TRC system, the laser pulse width was ~ 1 ns, and the time jitter of self-developed SPD was ~ 870 ps. Therefore, the performance of the TDC meets the requirements of the TRC system.

In experiment, the TRC system was located at the Lanxiang Lake in Shanghai, with strong wind and high humidity at night. The dark count rate of the SPD was ~ 200 cps, the dead time was 50 ns, and the detection efficiency at 850 nm was $\sim 45\%$. According to the analysis of coding in Section 2.2, the length of the original PN sequence is 32 chips. In order to avoid the

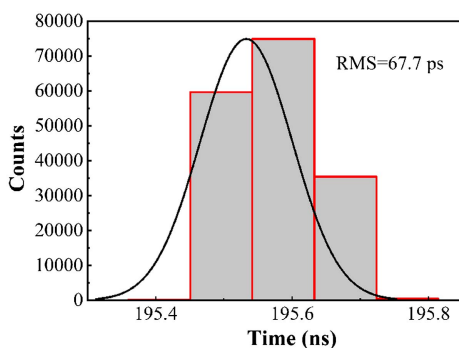


Fig. 4. TDC performance test.

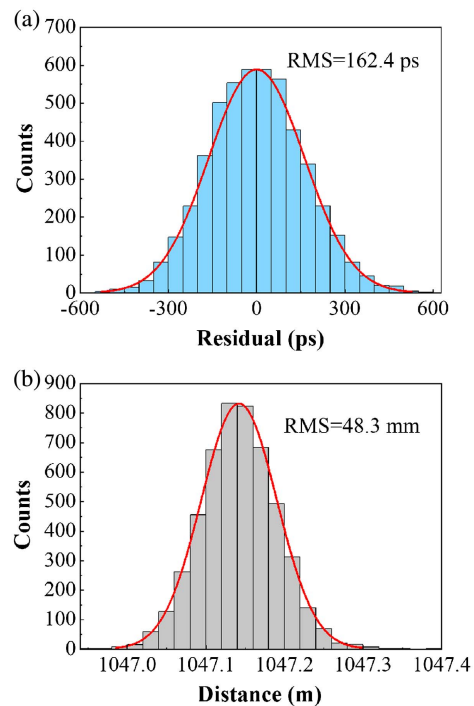


Fig. 5. (a) Time comparison results. (b) Statistical histogram of distance measurement.

influence of dead time, “0” is inserted after each chip of the original PN sequence to form a spread spectrum sequence with a length of 64 chips. The sampling time of single code was 80 ns, and the optical communication with data rate of ~ 195.3 kbit/s was realized. Due to the defects in our darkroom design, the street lights by the lake were bright at night, resulting in 3×10^4 cps background noise. We compared 5000 groups of data when the received signal intensity was 1.4 photons per pulse at each site. The time comparison results after removing the cable delay are shown in Fig. 5(a). The precision of time comparison is expressed by the standard deviation of multiple measurement results under the same conditions, so the time comparison precision in this TRC system was 162.4 ps. The statistical histogram of distance measurement is shown in Fig. 5(b), the average value of distance measurement was 1047.14 m, and the ranging uncertainty was 48.3 mm. The BER of the TRC system was 7.7×10^{-5} , which was consistent with the theoretical BER of 3.7×10^{-5} calculated by Eq. (7) under the same conditions. Therefore, the TRC system is valid and feasible in both theory and practice.

4. Conclusion

In this paper, a portable system of TRC integration based on single-photon detection is demonstrated. The current demonstration distance is a 1.05 km asynchronous two-way link. A PN sequence with a period of 32 chips is used for the spread spectrum. The data rate of optical communication is ~ 195.3 kbit/s,

and the BER of 7.7×10^{-5} is realized under the condition of 3×10^4 cps background noise and the signal light intensity of 1.4 photons per pulse at the receiver. The ranging uncertainty is 48.3 mm, and the precision of time comparison is 162.4 ps under the comparison of 5000 groups of data. The transmitter is a vertical-cavity surface-emitting laser (VCSEL) LD with a power of about 9.1 μ W in this TRC system, and the equivalent receiving aperture is 0.5 mm. In the Taiji project for space gravitational wave detection, the arm length in space is 3 million kilometers. Take a telescope with 100 mm aperture for example. When the signal light intensity is 1.4 photons per pulse at the receiver, the laser power emitted only needs ~ 130 mW to realize 3 million kilometers time comparison, absolute distance measurement, and optical communication through this TRC system^[30]. In the succeeding work, the performance of the TRC system can be greatly improved by using an ultra-stable narrow pulse width laser, high-precision TDC, and SPD.

Acknowledgement

This work was supported by the National Natural Science Foundation of China (Nos. 11804099, 62075062, 62175067, and 11621404) and Research Funds of Happiness Flower ECNU (No. 2021ST2110).

References

1. A. Einstein, "Approximate integration of the field equations of gravitation," *Sitzungsber. K. Preuss. Akad. Wiss.* **1**, 688 (1916).
2. V. Connaughton, E. Burns, A. Goldstein, L. Blackburn, M. S. Briggs, B.-B. Zhang, J. Camp, N. Christensen, C. M. Hui, P. Jenke, T. Littenberg, J. E. McEnery, J. Racusin, P. Shawhan, L. Singer, J. Veitch, C. A. Wilson-Hodge, P. N. Bhat, E. Bissaldi, W. Cleveland, G. Fitzpatrick, M. M. Giles, M. H. Gibby, A. von Kienlin, R. M. Kippen, S. McBreen, B. Mailyan, C. A. Meegan, W. S. Paciesas, R. D. Preece, O. J. Roberts, L. Sparke, M. Stanbro, K. Toelge, and P. Veres, "Fermi GBM observations of LIGO gravitational wave event GW150914," *Astrophys. J. Lett.* **6**, 826 (2016).
3. Z. Luo, S. Bai, X. Bian, G. Chen, P. Dong, Y. Dong, W. Gao, X. Gong, J. He, H. Li, X. Li, Y. Li, H. Liu, M. Shao, T. Song, B. Sun, W. Tang, P. Xu, S. Xu, R. Yang, and G. Jin, "Gravitational wave detection by space laser interferometry," *Adv. Mech.* **43**, 415 (2013).
4. M. Pitkin, S. Reid, S. Rowan, and J. Hough, "Gravitational wave detection by interferometry (ground and space)," *Living Rev. Relativ.* **14**, 5 (2011).
5. J. R. Gair, M. Vallisneri, S. L. Larson, and J. G. Baker, "Testing general relativity with low-frequency, space-based gravitational-wave detectors," *Living Rev. Relativ.* **16**, 7 (2013).
6. G. Wang, Z. Li, J. Huang, H. Duan, X. Huang, H. Liu, Q. Liu, S. Yang, L. Tu, and H. Yeh, "Analysis and suppression of thermal effect of an ultra-stable laser interferometer for space-based gravitational waves detection," *Chin. Opt. Lett.* **20**, 011203 (2022).
7. D. Sweeney and G. Mueller, "Experimental verification of clock noise transfer and components for space based gravitational wave detectors," *Opt. Express* **20**, 25603 (2012).
8. R. Gao, H. Liu, Y. Zhao, Z. Luo, J. Shen, and G. Jin, "Laser acquisition experimental demonstration for space gravitational wave detection missions," *Opt. Express* **29**, 6368 (2021).
9. K. Danzmann and The LISA Study Team, "LISA: laser interferometer space antenna for gravitational wave measurements," *Class. Quant. Grav.* **13**, A247 (1996).
10. S. Babak, J. Gair, A. Sesana, E. Barausse, C. F. Sopuerta, C. P. L. Berry, E. Berti, P. Amaro-Seoane, A. Petiteau, and A. Klein, "Science with the space-based interferometer LISA. V. Extreme mass-ratio inspirals," *Phys. Rev. D* **95**, 103012 (2017).
11. M. Y. M. Lau, I. Mandel, A. Vigna-Gómez, C. J. Neijssel, S. Stevenson, and A. Sesana, "Detecting double neutron stars with LISA," *Mon. Not. R. Astron. Soc.* **492**, 3061 (2020).
12. K. Danzmann and A. Rüdiger, "LISA technology-concept, status, prospects," *Class. Quant. Grav.* **20**, S1 (2003).
13. M. Armano, H. Audley, G. Auger, J. T. Baird, M. Bassan, P. Binetruy, M. Born, D. Bortoluzzi, N. Brandt, M. Caleno, L. Carbone, A. Cavalleri, A. Cesarini, G. Ciani, G. Congedo, A. M. Cruise, K. Danzmann, M. de Deus Silva, R. De Rosa, M. Diaz-Aguiló, L. Di Fiore, I. Diepholz, G. Dixon, R. Dolesi, N. Dunbar, L. Ferraioli, V. Ferroni, W. Fichter, E. D. Fitzsimons, R. Flatscher, M. Freschi, A. F. G. Marín, C. G. Marrodriga, R. Gerndt, L. Gesa, F. Gibert, D. Giardini, R. Giusteri, F. Guzmán, A. Grado, C. Grmani, A. Grynagier, J. Grzymisch, I. Harrison, G. Heinzel, M. Hewitson, D. Hollington, D. Hoyland, M. Hueller, H. Inchauspé, O. Jennrich, P. Jetzer, U. Johann, B. Johlander, N. Karnesis, B. Kaune, N. Korsakova, C. J. Killow, J. A. Lobo, I. Lloro, L. Liu, J. P. López-Zaragoza, R. Maarschalkwerd, D. Mance, V. Martín, L. Martin-Polo, J. Martino, F. Martin-Porqueras, S. Madden, I. Mateos, P. W. McNamara, J. Mendes, L. Mendes, A. Monsky, D. Nicolodi, M. Nofrarias, S. Paczkowski, M. Perreux-Lloyd, A. Petiteau, P. Pivato, E. Plagnol, P. Prat, U. Ragnit, B. Raï, J. Ramos-Castro, J. Reiche, D. I. Robertson, H. Roze-meijer, F. Rivas, G. Russano, J. Sanjuán, P. Sarra, A. Schleicher, D. Shaul, J. Slutsky, C. F. Sopuerta, R. Stanga, F. Steier, T. Sumner, D. Texier, J. I. Thorpe, C. Trenkel, M. Tröbs, H. B. Tu, D. Vetrugno, S. Vitale, V. Wand, G. Wanner, H. Ward, C. Warren, P. J. Wass, D. Wealthy, W. J. Weber, L. Wissel, A. Wittchen, A. Zambotti, C. Zanoni, T. Ziegler, and P. Zweifel, "Sub-femto-g free fall for space-based gravitational wave observatories: LISA pathfinder results," *Phys. Rev. Lett.* **116**, 231101 (2016).
14. W. Hu and Y. Wu, "The Taiji Program in Space for gravitational wave physics and the nature of gravity," *Natl. Sci. Rev.* **4**, 685 (2017).
15. Z. Luo, Z. Guo, and G. Jin, "A brief analysis to Taiji: science and technology," *Results Phys.* **16**, 102918 (2020).
16. Z. Luo, Y. Wang, and Y. Wu, "The Taiji program: a concise overview," *Prog. Theor. Exp. Phys.* **2021**, 05A108 (2021).
17. LISA Frequency Control Study Team, ESA Report No. LISA-JPL-TN-823 (2009).
18. S. E. Pollack and R. T. Stebbins, "A demonstration of LISA laser communication," *Class. Quant. Grav.* **23**, 4201 (2006).
19. J. J. Esteban, A. F. García, S. Barke, A. M. Peinado, F. G. Cervantes, I. Bykov, G. Heinzel, and K. Danzmann, "Experimental demonstration of weak-light laser ranging and data communication for LISA," *Opt. Express* **19**, 15937 (2011).
20. T. S. Schwarze, G. F. Barranco, D. Penkert, M. Kaufer, O. Gerberding, and G. Heinzel, "Picometer-stable hexagonal optical bench to verify LISA phase extraction linearity and precision," *Phys. Rev. Lett.* **122**, 081104 (2019).
21. G. Heinzel, J. J. Esteban, S. Barke, M. Otto, Y. Wang, A. F. Garcia, and K. Danzmann, "Auxiliary functions of the LISA laser link: ranging, clock noise transfer and data communication," *Class. Quant. Grav.* **28**, 094008 (2011).
22. G. de Vine, B. Ware, K. McKenzie, R. E. Spero, W. M. Klipstein, and D. A. Shaddock, "Experimental demonstration of time-delay interferometry for the laser interferometer space antenna," *Phys. Rev. Lett.* **104**, 211103 (2010).
23. J. J. Degnan, "Asynchronous laser transponders for precise interplanetary ranging and time transfer," *J. Geodyn.* **34**, 551 (2002).
24. W. Meng, Y. Wang, K. Tang, Z. Zhang, S. Jin, I. Procházka, Z. Zhang, and G. Wu, "High-precision single-photon laser time transfer with temperature drift post-compensation," *Sensors* **20**, 6655 (2020).
25. J. Blazej, I. Procházka, J. Kodet, and P. Linhart, "Indoor demonstration of free-space picosecond two-way time transfer on single photon level," *Proc. SPIE* **9224**, 92241E (2014).
26. D. Wu, L. Yang, X. Chen, Z. Li, and G. Wu, "Multi-channel pseudo-random coding single-photon ranging and imaging," *Chin. Opt. Lett.* **20**, 021202 (2022).

27. D. Shin, F. Xu, D. Venkatraman, R. Lussana, F. Villa, F. Zappa, V. K. Goya, F. N. Wong, and J. H. Shapiro, "Photon-efficient imaging with a single-photon camera," *Nat. Commun.* **7**, 12046 (2016).
28. G. Wen, J. Huang, L. Zhang, C. Li, T. Wen, and J. Wang, "A high-speed and high-sensitivity photon-counting communication system based on multi-channel SPAD detection," *IEEE Photon. J.* **13**, 7900310 (2021).
29. B. Du, Y. Wang, E. Wu, X. Chen, and Guang Wu, "Laser communication based on a multi-channel single-photon detector," *Opt. Commun.* **426**, 89 (2018).
30. Z. Wang, W. Sha, Z. Chen, Y. Kang, Z. Luo, M. Li, and Y. Li, "Generation of vector beams in planar photonic crystal cavities with multiple missing-hole defects," *Chin. Opt.* **11**, 131 (2018).